JOURNAL OF
APPLIED FIRE SCIENCE

EXECUTIVE EDITOR: PAUL R. DeCICCO

Volume 12, Number 1 – 2003-2004

Nonlinear Thin Shell Finite Element for Steel and Concrete Structures Subjected to Fire: Verification and Validation

Didier Talamona, Sylvie Castagne, and Jean-Marc Franssen

BAYWOOD PUBLISHING COMPANY, INC.
26 Austin Avenue, PO Box 337, Amityville, NY 11701
call (631) 691-1270 • **fax** (631) 691-1770 • **toll-free orderline** (800) 638-7819
e-mail: baywood@baywood.com • **web site:** http://baywood.com

J. APPLIED FIRE SCIENCE, Vol. 12(1) 65-81, 2003-2004

NONLINEAR THIN SHELL FINITE ELEMENT FOR STEEL AND CONCRETE STRUCTURES SUBJECTED TO FIRE: VERIFICATION AND VALIDATION*

DIDIER TALAMONA
FireSERT, University of Ulster, United Kingdom

SYLVIE CASTAGNE
CEIAT, Queen's University Belfast, United Kingdom

JEAN-MARC FRANSSEN
M&S, University of Liege, Belgium

ABSTRACT

This article presents verification and validation examples for a nonlinear thin shell element developed for structures subjected to fire. The verification benchmarks are: a Z-shaped cantilever, a twisted cantilever beam, a hemispherical shell, and Lee's frame at room temperature and at elevated temperature. The element shows that it provides results in good agreement with theoretical results and other finite elements. The validation calculations have been preformed on an H rolled profile and a concrete slab. The element demonstrates its ability to reproduce local buckling on a H-steel beam under fire conditions and that it predicts accurately the failure of a concrete slab subjected to fire. The theoretical development of this finite element has been published in the *Journal of Applied Fire Science*, Vol. 11, No. 4, pp. 291-310, "Nonlinear Thin Shell Finite Element for Steel and Concrete Structures Subjected to Fire: Theoretical Development."

*This work has been supported by the European Commission through the *Marie Curie* fellowship granted to Dr. Talamona (contract number ERBFMBICT983336).

INTRODUCTION

There is sometimes confusion between verification and validation. It is true that there is no standard definition regarding these words when they are applied to finite element methods but it is common to use the following definitions: "Verification demonstrates that you are solving the equations right. Validation demonstrates that you are solving the right equations." In other words when a finite element is verified, it means that it has been checked that it gives correct results when compared to theoretical results. The validation consists of checking if the physical approximations (usually the contribution of some terms of theoretical equations are neglected because their contribution to the final result is very small and they may produce a system of equations which is impossible to solve) used are able to reproduce physical phenomena observed during experiments.

Nowadays commercial finite element programs are extensively used to justify the fire resistance of structures. According to the manuals of these programs it is almost possible to model everything but when specific calculations have to be performed there is usually a lack of information concerning the limit of the software and the validity of the results. Moreover it is usually impossible to find neither verification nor validation examples. For these reasons the user should first check the ability of his software to predict the behavior of structures subjected to fire with experimental results and then establish the limits of its model. It is essential to check that the results of the computation of the model are on the safe side.

SAFIR is a finite element program developed by Franssen in the 90's. This program is dedicated to thermal and mechanical analysis of structures under fire conditions. The results of thermal calculations can easily be linked and used as input for the structural analysis. The mechanical analysis is performed in a step-by-step procedure consisting of subsequent static analyses or of a dynamic analysis, using the input temperatures. This procedure allows modeling of the mechanical behavior of a structure during the different stages of the fire (pre-flashover, post-flashover, and decay.)

The shape of civil engineering structures can usually be split into a set of lines (beams and columns) and planes (slabs, walls, partitions, etc.) These simple shapes can be meshed using beams, trusses, and shells finite elements. To improve SAFIR's capabilities a quadrilateral thin shell element has been implemented in it. This element has originally been developed for the room temperature program FINELG [1-15] (University of Liege). It has received the required modifications needed for high temperature simulations. 2-D stress-strain relationships for steel (according to Eurocode 3 part 1.2 [16]) and concrete [17, 18] (according to Eurocode 2 part 1.2 [19]) have been implemented (see companion article entitled: "Nonlinear Thin Shell Finite Element for Steel and Concrete Structures Subjected to Fire: Theoretical Development"). Some verification and validation examples are presented in this article.

NUMERICAL VERIFICATION AND VALIDATION

Except when specified otherwise, all the data given in this section are consistent, i.e., they can be expressed in any system of units, provided that a single system is used for each example. Whether the data are expressed in the international or in an Anglo-American system of units does not matter, the numbers that form results will be the same, expressed in the relevant system.

Patch Tests

The element has shown that it passes the patch tests (see companion article: "Nonlinear Thin Shell Finite Element for Steel and Concrete Structures Subjected to Fire: Theoretical Development").

Response of an Elastic Z-Shaped Cantilever at Room Temperature

The structure is a Z-shaped cantilever subjected to a transverse end load (Figure 1). The solution given in reference [20] is based on nine equal sized elements. The structure is oriented at 45° from the x-z plane to activate all three translations and rotations in the element formulation. The beam is divided into three equal parts (each part is meshed with three elements). The two parts parallel to the x-y plane have a length of 60 and a width of 20. The middle part (inclined) has also a length of 60 and an elevation of 30 in the z-direction, the width is 20. The thickness of the beam is 1.7. All the six degrees of freedom are restrained at one end and two concentrated nodal forces are applied in the positive z-direction at the other end. The load is increased up to 4000 with a step of 10. The material is elastic, the Young's modulus is equal to 2.0×10^5 and Poisson's ratio is equal to 0.3. This problem is solved at room temperature (20°C).

Two calculations have been performed, the first one "SAFIR 10" with a load increment of 10, to check that SAFIR gives the same continuous curve as the one given by NAFEMS (National Agency for Finite Element Method & Standards). The second one ("SAFIR 500") has a larger load increment (of 500) to check whether SAFIR is able to manage large load and/or displacement increments between each step. It can be seen on Figure 1 (displacements not amplified) and Figure 2 that the element introduced in SAFIR gives good results in case of bending with large geometric non-linear behavior. The results obtained for a load step of 500 ("SAFIR 500") are also very good even if the first point is a little bit too high compared to the two other curves. It has to be realized that a displacement of nearly 125 has been accommodated within one single step.

Twisted Cantilever Beam at Room Temperature

This example (see Figure 3) has been defined in [21] and, since 1985, is one of the most widely used benchmark tests for testing the effects of warping in

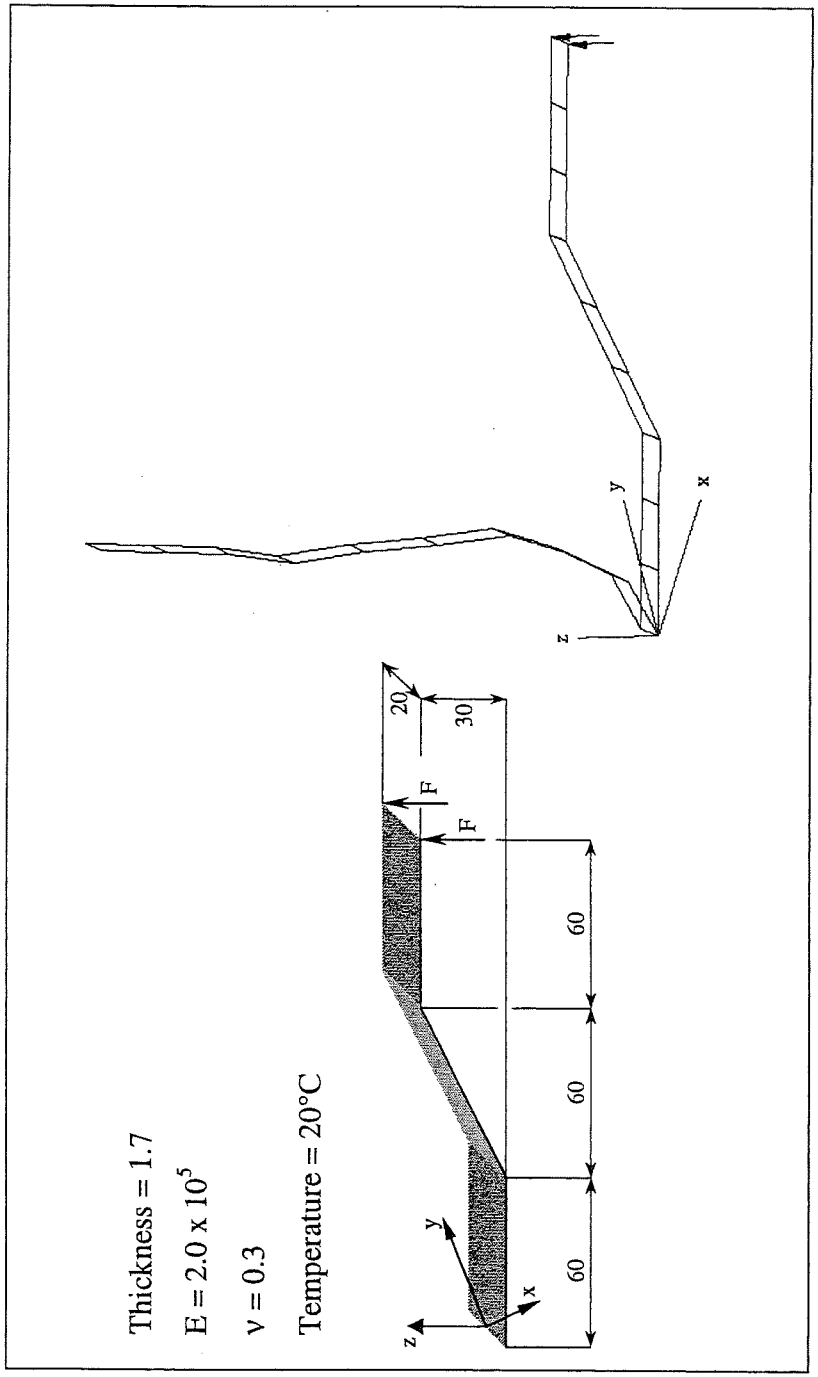

Figure 1. Initial geometry and deformed shape for a load of 4000.

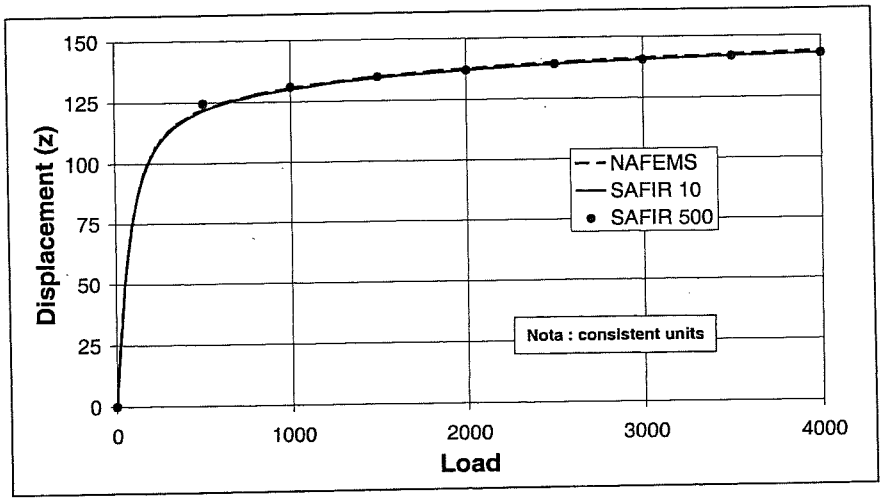

Figure 2. Load/displacement for the Z shape.

quadrilateral elements. Whereas the length of the beam is 12 and the width of the section is 1.1, the test is usually run for two different thicknesses of the section, namely 0.32 and 0.0032 with a Young's modulus equal to 29×10^6 and a Poisson's ratio of 0.22. The concentrated forces are either applied in the X (see Figure 3) or in the Y direction.

The thickness of 0.32 is used to check the correctness of the formulation of the shell element and the thickness of 0.0032 is used to check the element against membrane locking. Tables 1 and 2 show the displacements obtained at the loaded extremity of the beam for the crude mesh based on 6 finite elements as shown on Figure 3. Also mentioned in these tables are the results presented in [22]. Here again, in order to allow comparison for the benchmark example presented in small displacements, the results of SAFIR are those obtained after a single iteration. The differences between the exact solutions and the numerical simulations are in a range of 1 to 5%.

Elastic Hemispherical Shell at Room Temperature

A hemispherical shell (radius = 10 and thickness = 0.04) is subjected to concentrated loads acting at its bottom (Figure 4). As the structure has a double symmetry, only 1/4 of the hemispherical [20] has been meshed using 16 × 16 quadrilateral elements (Figure 4). Symmetrical boundary conditions have been used on the plane $y = 0$, i.e., $U_y = \theta_x = \theta_z = 0$ and on the plane $x = 0$, i.e., $U_x = \theta_y = \theta_y = 0$. To prevent the rigid body mode in the z-direction, the point **A** was restrained to have x-translations only, i.e., $U_z = 0$.

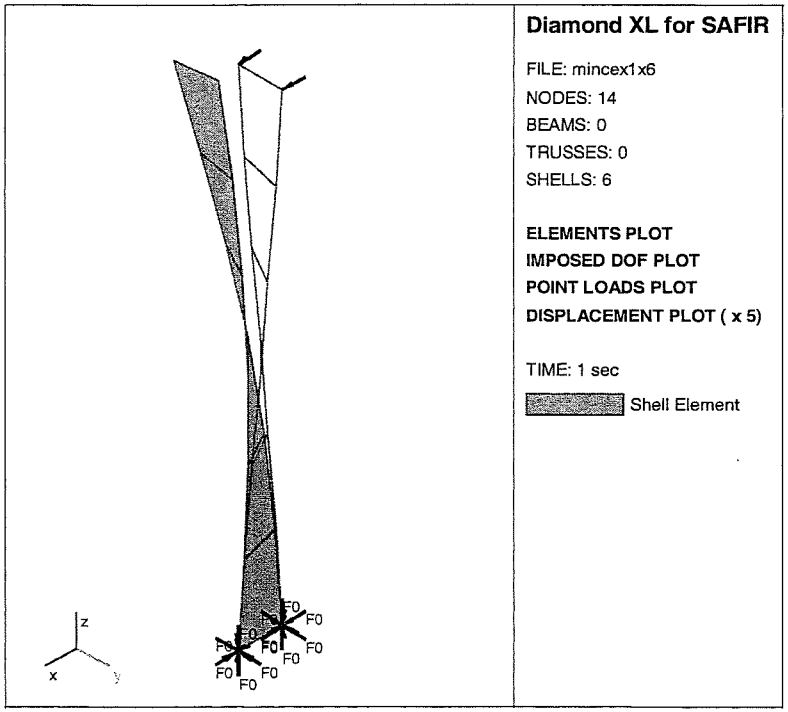

Figure 3. Twisted cantilever beam.

Inward and outward diametrical point loads were applied as concentrated nodal forces at locations **A** and **B** respectively. The loads are increased up to a maximum of 100. The material is elastic, the Young's modulus is equal to 6.825×10^7 and Poisson's ratio is equal to 0.3. This problem is solved at ambient temperature (20°C).

This problem tests the performance of the geometric non-linear formulation for shells under membrane, bending and twisting actions. It can be seen (Figure 5) that SAFIR gives good results in case of large rotations and deflections. For the inward displacement, SAFIR is stiffer than the results obtained by NAFEM [20], but the results are close to the ones obtained by Simo. This test confirms that there is no membrane locking in the element.

Lee's Frame

This example has been chosen because the results have been presented for five different computer codes using beam finite elements, at room temperature as well as under increasing temperature. The finite element mesh is shown on

Table 1. Results for the Twisted Cantilever Beam (h = 0.32)

	Py = 1		Px = 1	
	Uy	Ux	Uy	Ux
Exact	0.00542	0.00172	0.00179	0.00175
SAFIR	0.00533 (0.983)	0.0017 (0.988)	0.00170 (0.950)	0.00172 (0.983)
[22]	0.00521 (0.961)	— —	— —	0.00144 (0.823)

Table 2. Results for the Twisted Cantilever Beam (h = 0.0032)

	Py = 1		Px = 1	
	Uy	Ux	Uy	Ux
Exact	5316	1878	1878	1296
SAFIR	5226 (0.983)	1858 (0.989)	1858 (0.989)	1281 (0.988)
[22]	5163 (0.971)	— —	— —	1251 (0.965)

Figure 6. The vertical and the horizontal members have a length of 120. Two meshes have been used to check the behavior in case of bending (shell elements in the x-y plane for the horizontal member and in the y-z plan for the vertical member) and in case of "membrane bending" (all the shell elements are in the x-z plane).

At the ends of the frame, the following displacements have been locked:

$$U_x = U_y = U_z = \theta_x = \theta_z = 0$$

The cross-section of the beam is equal to 6 and the inertia is equal to 2. Eight Gauss integration points are used through the thickness of the elements.

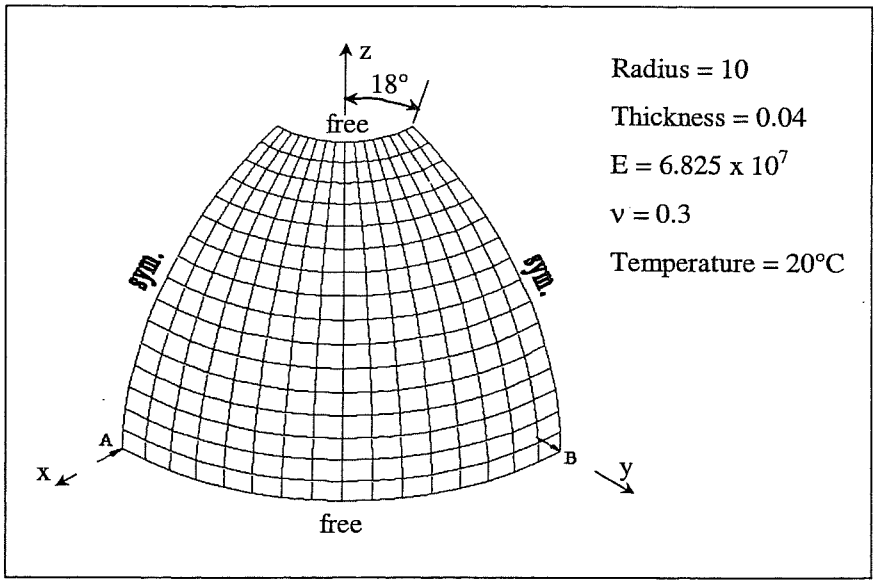

Figure 4. Hemispherical shell.

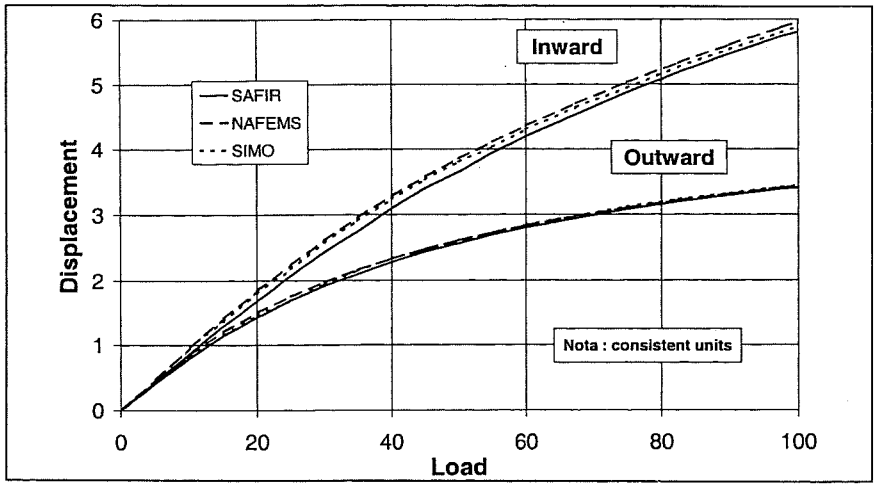

Figure 5. Inward and outward displacements.

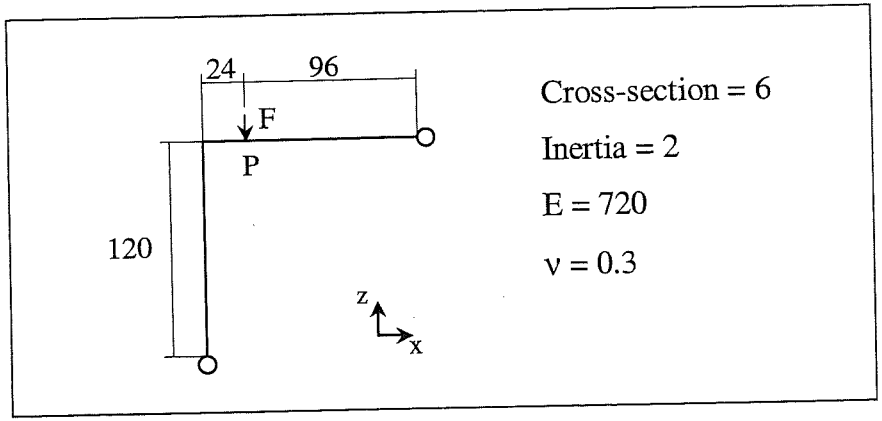

Figure 6. Lee's frame.

Ambient Temperature

A vertical load is applied at a distance of 96 of the top right edge (point P) and it is increased until collapse. The material is elastic, the Young's modulus is equal to 720 and Poisson's ratio is equal to 0.3.

A comparison with the results of other finite element programs that use beam elements [23] has been performed. It can be seen (Figure 7) that in the case of bending (SAFIR-Bending) the shell element of SAFIR gives results close to the beam elements. In the case of "membrane bending" (SAFIR-Membrane-Bending) the shell element is a little bit stiffer, but the mesh used here is very crude (2 elements on the depth of the beam).

Elevated Temperature

This example has been described in the companion article: "Nonlinear Thin Shell Finite Element for Steel and Concrete Structures Subjected to Fire: Theoretical Development." It has been shown that the shell element behave well when compared with beam elements.

Figure 8 shows the horizontal displacement at point P (application of the load F) as function of the temperature of the frame. In a first step the load is applied to the structure and it generates a positive horizontal displacement of P. Then the temperature in the structure is increased and the members expand. This expansion generates a negative horizontal displacement of P. When the temperature reaches 520°C the structure starts to collapse on itself (see deformed shape Figure 9).

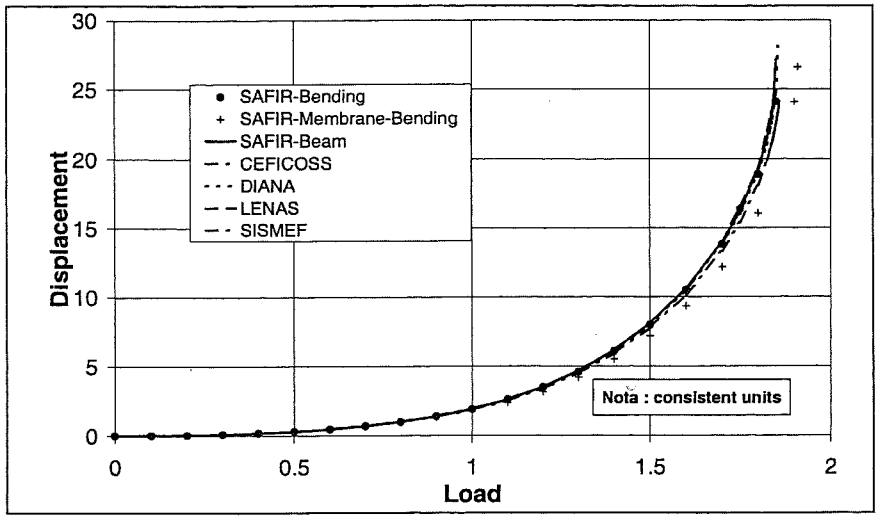

Figure 7. Horizontal displacement versus load.

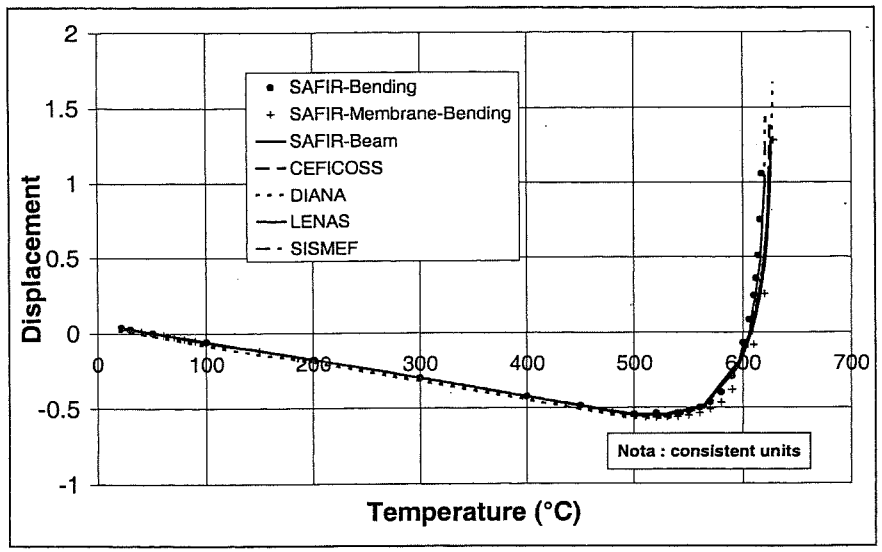

Figure 8. Horizontal displacement versus temperature.

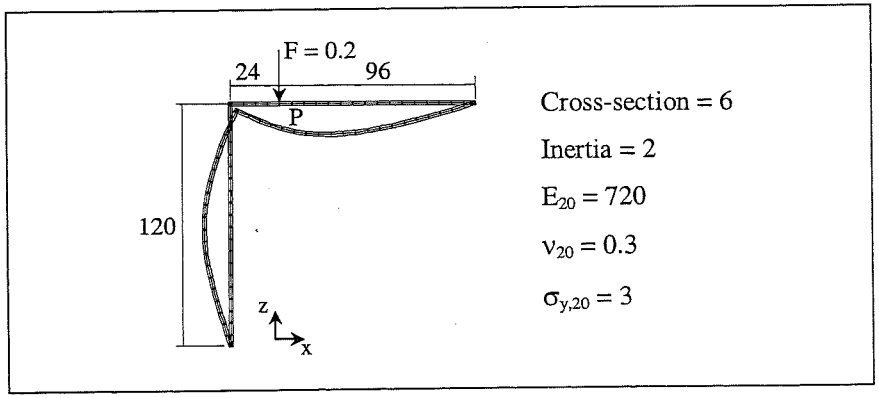

Figure 9. Initial geometry and deformed shape at collapse temperature.

H Rolled Profile

Calculations have been performed on a S355 HE 300 AA+. The length of the short beam is 1 m. The boundary conditions are defined as follow:

First end: All the nodes are locked on the longitudinal displacement and the three rotations are also locked. The lateral displacement is locked at all the nodes on the web and all the displacements are locked at the point in the middle of the web.

Second end: All the nodes have an imposed longitudinal displacement in compression and all the rotations are locked. The lateral displacement is locked at all the nodes on the web and all the displacements are locked at the point in the middle of the web.

An initial sinusoidal imperfection (maximal magnitude = 10 mm) is imposed on the web and the flanges. The temperature is uniform in the structure and it is increased at the same time as the displacement is increased.

In this structure, the stress is a function of the imposed longitudinal displacement and of the thermal strain (restrained). As the temperature and the displacement are increased at the same time, the maximum reaction force occurs when the temperature of the structure reaches 42°C and the longitudinal displacement is equal to 1.8 mm. The ratio between the maximum load applied to the structure and the theoretical crushing compressive load is equal to 0.92. As the calculation has been performed with imposed displacements, post-critical behavior can be studied easily. Figure 10 shows the deformation of the beam when the simulation was stopped (displacements not amplified). Large deformations have been obtained in the middle of the beam. The temperature in the structure at

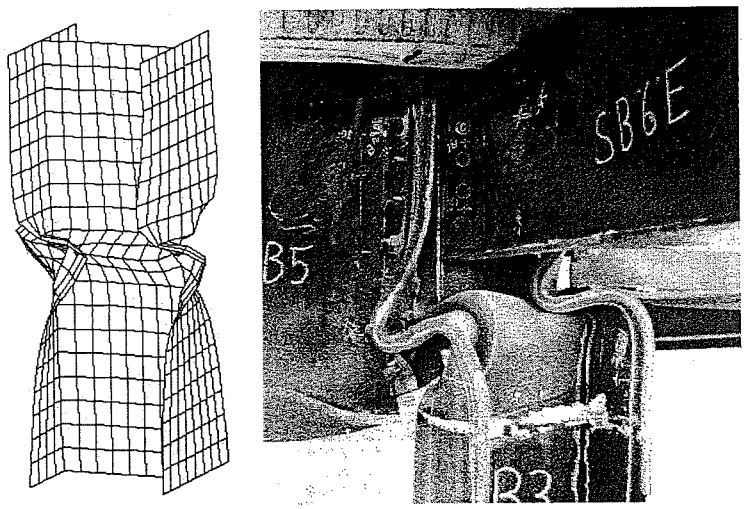

Figure 10. Deformed profile and local buckling of a structure subjected to fire (Cardington).

this moment is 1000°C and the imposed shortening is equal to 81 mm. As can be seen on Figure 10 the local buckling obtained by calculation has the same shape as the one obtained during an experimental test (Cardington).

Concrete Slab

The performance of the shell element with concrete material properties is compared with experimental fire tests of two-way concrete slabs conducted at a fire resistance furnace in New Zealand, Lim [17], and Lim et al. [18].

Six two-way slabs comprising reinforced concrete flat slabs and composite steel-concrete slabs were tested. They were simply supported at all four edges and were axially unrestrained. They were loaded with a live load of 3.0 kPa while being exposed to the ISO fire from below for 3 hours. All the slabs supported the loads for the entire fire duration without collapse, despite suffering large midspan vertical deflections (up to 270 mm).

The modeling of one of the tested slabs is presented here and is based on work by Lim [17]. The geometry and material properties of the finite element model are shown in Table 3 and are based on the tested slab. The reinforcing steel and concrete material properties used in the model were based on the Eurocode 2 part 1.2 [19]. Different values of concrete tensile strength were used in the analyses, ranging from 0 MPa (fully cracked) to 3.0 MPa ($0.5\sqrt{f'_c}$).

Table 3. Properties of the Tested Slab

Clear span in long direction, L_y	4.16 m
Clear span in short direction, L_x	3.16 m
Slab thickness, h	100 mm
Concrete compressive strength, f'_c	36 MPa
Concrete cover, c_c	25 mm
Reinforcing mesh	198 mm^2/m in both directions (Ø8.7 @ 300 mm)
Yield strength (ambient temperature), $f_{y,o}$	565 MPa
Self weight	2.4 kPa
Live load	3.0 kPa

Figure 11 compares experimental results with computations. SAFIR analysis was conducted with different values of concrete tensile strength, respectively 0.0 MPa, 1.5 MPa, and 3.0 MPa. The displacement transducer malfunctioned after 140 minutes and the deflection of the slab had to be measured manually at the end of the test.

The graph shows that with zero tensile strength in the concrete, SAFIR predicted slightly larger deflections than the experimental results throughout the entire fire duration. Nevertheless, the deflection trend predicted by SAFIR was very similar to the experimental results, showing a high deflection rate during the first 30 minutes, followed by a gradual deflection rate up to 150 minutes and finally increasing again from 150 minutes to 180 minutes. The SAFIR analysis stopped at 189 minutes when the reinforcing steel rebars at mid-span ruptured. The larger deflections predicted by SAFIR, with zero concrete tensile strength, were attributed to the slab being fully cracked and being more flexible than the tested slab. The high fire resistance of this lightly reinforced slab was attributed to the loads being resisted by tensile membrane action instead of bending action.

With a concrete tensile strength of 1.5 MPa, SAFIR showed good agreement with the tested slab throughout the entire fire duration. SAFIR predicted low deflections before the fire started, when the concrete was uncracked, followed by thermal bowing deflections during the initial stages of the fire, leading to final failure of the slab at 192 minutes.

With a concrete tensile strength of 3 MPa, the deflections predicted by SAFIR showed good agreement with the experimental test results during the first 100 minutes. Beyond that, the deflections started to diverge as the predicted deflection increase linearly at a low rate to reach –0.20 meter at 210 minutes. During experiment an increasing deflection rate was observed after 150 minutes. It shows

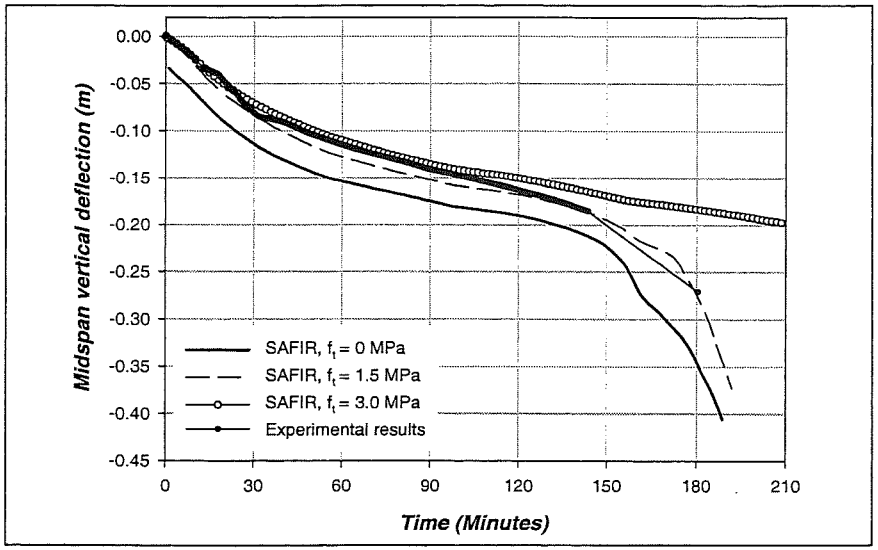

Figure 11. Comparison of experimental results versus SAFIR analyses.

that the concrete model is very ductile when high values of concrete tensile strength are used as the concrete does not crack and deflect sufficiently at the later stages of the fire.

Figure 12 shows the distribution of the principal membrane forces in 1/4 of slab. The membrane forces were plotted at the surface integration points of the slabs. The dark lines represent compressive forces while the light lines represent tension forces. Figure 12 shows that a compression ring had formed at the outer edges of the slab, surrounding a tension field at the mid-span region. These in-plane membrane forces are a result of the deflected shape of the slab. The tension field at mid-span is due to the large deflections while the compression ring at the outer edges is a result of the resistance of the outer edges against the inward contraction of the slab caused by the sagging mid-span deflections. The slab resists the loads as a membrane and will fail only when the steel at mid-span ruptures or when the concrete at the edges crushes. The calculated tensile membrane forces, instead of bending action, explain the high fire resistance reached by the slab. The failure predicted by SAFIR corresponds to the fracture of the reinforcing steel mesh. The slab will fail, as the tensile forces cannot be sustained by the structure any more. These phenomena are in good agreement with the ones observed during the fire test.

In this example, and in others that are presented in [17], the modeling by SAFIR generally agrees well with the experimental results which tends to

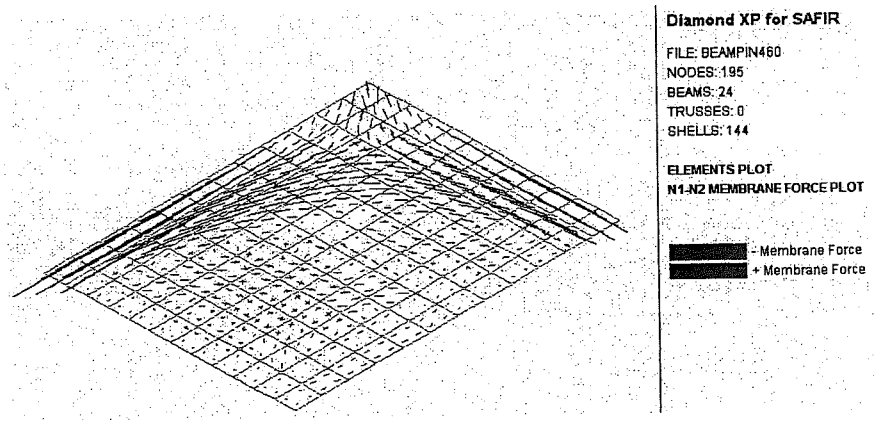

Figure 12. Distribution of principal membrane forces in the slab at failure.

prove that the element and the utilized material models are able to represent the behavior of reinforced concrete slabs undergoing very large transverse displacements in fire.

CONCLUSION

The z-shape and the twisted cantilevers show that the element can be subjected to large geometric non-linear behavior. The hemispherical shell, the twisted beam (thickness of 0.0032), and the calculation performed on Lee's frame at ambient temperature show that this element is not subjected to membrane locking.

Lee's frame at elevated temperature demonstrates that the material properties from Eurocode 3 part 1.2 [16] have successfully been introduced in SAFIR in the case of plane stress relationship and that the thermal elongation is accurately taken into account.

The calculation performed on the H profile shows that the element is able to reproduce local buckling. Unfortunately, as no experimental data was available, this example shows only the ability of the element to reproduce local buckling. To validate the element in case of local buckling, specific experiments have to be performed.

To complete the validation of this element, more calculations have to be done for comparison with experimental tests.

Additional comparisons with experimental tests indicate the validity of the approach for reinforced concrete slabs submitted to large transverse displacements (note that more calculations have been performed by Lim [17]).

NOTATION

fy: ultimate strength at room temperature (for calculations at room temperature)
v: Poisson's coefficient (for calculations at room temperature)
E: Young's modulus at room temperature (for calculations at room temperature)
fy,20: ultimate strength at room temperature (for calculations at under fire conditions)
v,20: Poisson's coefficient at room temperature (for calculations at under fire conditions)
E20: Young's modulus at room temperature (for calculations at under fire conditions)

REFERENCES

1. FINELG – Nonlinear Finite Element Analysis Program – User's Manual Version 6.2 – Feb. 1984.
2. Jetteur Ph. – Non-Linear Shell Elements Based on Marguerre Theory – IREM Internal Report 85/5 – Swiss Federal Institute of Technology, Lausanne, Switzerland, Dec. 1985.
3. Jetteur Ph. – A Shallow Shell Element with in-Plane Rotational Degrees of Freedom – IREM Internal Report 86/3 – Swiss Federal Institute of Technology, Lausanne, Switzerland, March 1986.
4. Jetteur Ph. – Improvement of the Quadrangular "JET" Shell Element for a Particular Class of Shell Problems – IREM Internal Report 87/1 – Swiss Federal Institute of Technology, Lausanne, Switzerland, Feb. 1987.
5. Jaamei S., Frey F., Jetteur Ph. – Elément Fini de Coque Mince Non-Linéaire à Six Degrés de Liberté par Noeud – IREM Internal Report 87/10 – Swiss Federal Institute of Technology, Lausanne, Switzerland, Nov. 1987.
6. Allman D.J. – A Compatible Triangular Element Including Vertex Rotations for Plane Elastic Analysis – Comput. Struct., Vol. 19, 1984, pp. 1-8.
7. Jaamei S. – "JET" Thin Shell Finite Element with Drilling Rotations – IREM Internal Report 88/7 – Swiss Federal Institute of Technology, Lausanne, Switzerland, July 1988.
8. Idelsohn S. – Analyses Statique et Dynamique des Coques par la Méthode des Eléments Finis – Ph.D. thesis, Liege, 1974.
9. Batoz J.L., Bathe K.J., Ho L.W. – A Study of Three Node Triangular Plate Bending Elements – Int. J. Num. Meth. Eng., Vol. 15, pp. 1771-1812, 1980.
10. Batoz J.L. – An Explicit Formulation for an Efficient Triangular Plate Bending Element – Int. J. Num. Meth. Eng., Vol. 18, pp. 1077-1089, 1982.
11. Batoz J.L., Ben Tahar M. – Evaluation of a New Quadrangular Thin Plate Bending Element – Int. J. Num. Meth. Eng., Vol. 18, pp. 1655-1677, 1982.
12. Jetteur P., Frey F. – A Four Node Marguerre Elemeent for Non-linear Shell Analysis – Engineering Computations, Vol. 3, n 4, Dec, 1986, pp. 276-282.
13. Jaamei S., Frey F., Jetteur P. – Nonlinear Thin Shell Finite Element with Six Degrees of Freedom per Node – Computer Methods in Applied Mechanics and Engineering, Vol. 75, n 1-3, Oct. 1989, pp. 251-266.

14. Carpenter N., Stolarsky H., Belytschko T. – Flat Triangular Shell Element with Improved Membrane Interpolation – Communications in Applied Numerical Methods, Vol. 1, n 4, pp. 161-168, 1985.
15. Taylor R., Simo J.C. – Bending and Membrane Elements for Analysis of Thick and Thin Shell – Proceedings NUMETA 1985 Conference Swansea, pp. 587-591, 1985.
16. CEN ENV 1993-1-2, Eurocode 3, Design of Steel Structures, Part 1.2, General Rules, Structural Fire Design, European Committee for Standardization, Belgium, 1995.
17. Lim L. – Membrane action in fire exposed concrete floor systems. – Ph.D. thesis, Department of Civil Engineering, University of Canterbury, New Zealand, 2003.
18. Lim L., Buchanan A., Moss P. – Behaviour of Simply-Supported Two-Way Reinforced Concrete Slabs in Fire, Proc. "Designing Structure for Fire," SFPE, pp. 227-236, 2003.
19. CEN ENV 1992-1-2, Eurocode 2, Design of Concrete Structures, Part 1.2, General Rules, Structural Fire Design, European Committee for Standardization, Belgium, 1994.
20. Prinja N.K., Clegg R.A. – Assembly Benchmark Tests for 3-D Beams and Shells Exhibiting Geometric Non-Linear Behaviour – NAFEMS 1993 – Ref.: R0029.
21. MacNeal, R.J., Harder, R.L. – A proposed standard set of problems to test finite element accuracy – Finite Elements in Analysis and Design, Vol. 1, pp. 3-20, 1985.
22. Batoz, J.L, Dhatt, G. – Modélisation des structures par éléments finis. Volume 3. Coques – Hermès, Paris, 1990.
23. Franssen J.M. et al. – A Comparison between Five Structural Fire Codes Applied to Steel Elements – IAFSS, Fire Safety Science, Proceedings of the Fourth International Symposium, 1984.

Direct reprint requests to:

Dr. Didier Talamona
FireSERT, University of Ulster
Shore Road
Newtownabbey, BT37 0QB
UK, N. Ireland
e-mail: d.talamona@ulster.ac.uk